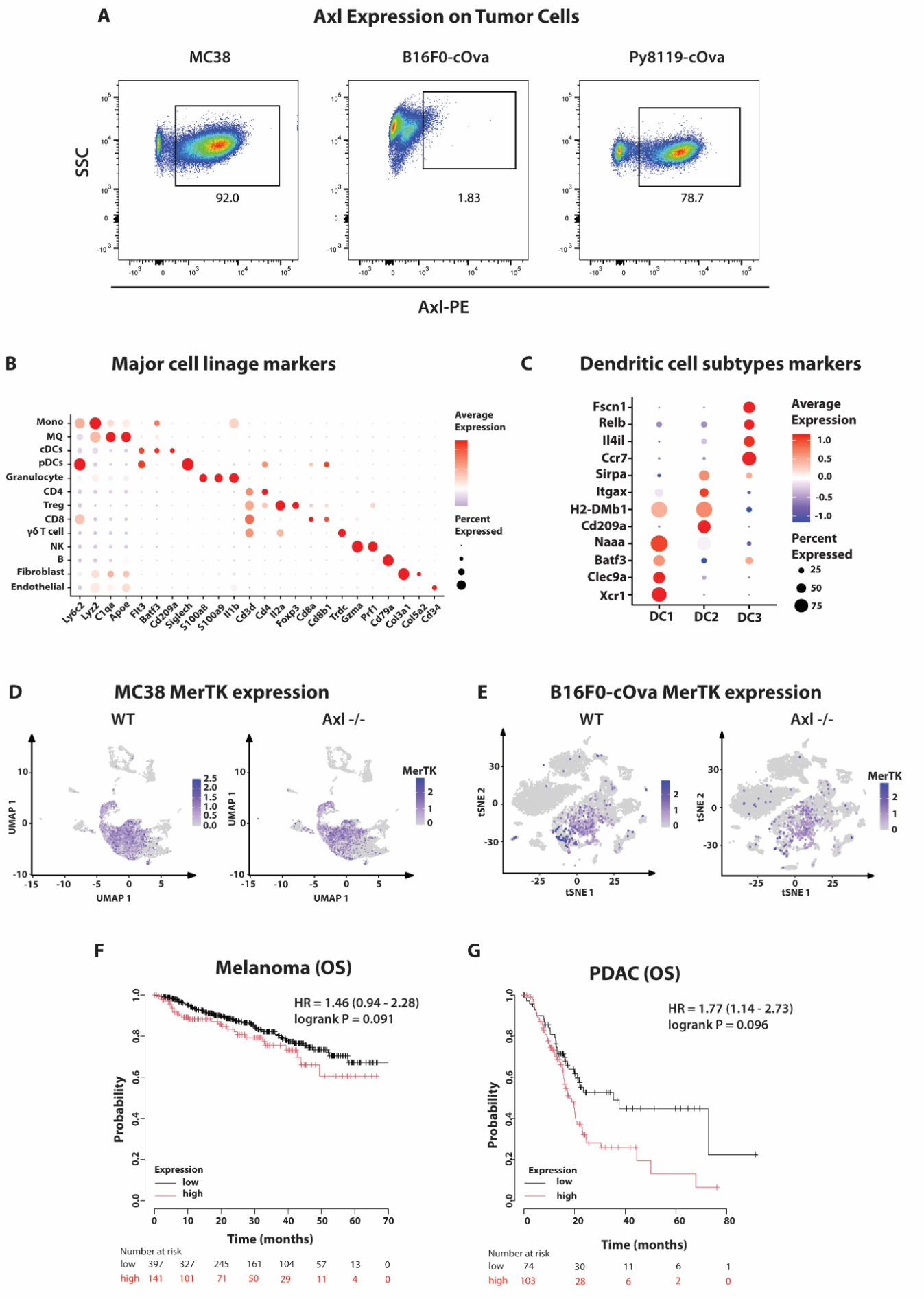
A
Axl Expression on Tumor Cells
MC38
B16F0-cOva
Py8119-cOva
SSC
92.0
1.83
78.7
Axl-PE
B
Major cell linage markers
Mono
MQ
cDCs
pDCs
Granulocyte
CD4
Treg
CD8
γδ T cell
NK
B
Fibroblast
Endothelial
Ly6c2
Lyz2
C1qa
Apoe
Fit3
Batf3
Cd209a
Siglech
S100a8
S100a9
Il1b
Cd3d
Cd4
Il2a
Foxp3
Cd8a
Cd8b1
Trdc
Gzma
Prf1
Cd79a
Col3a1
Col5a2
Cd34
Average Expression
Percent Expressed
C
Dendritic cell subtypes markers
Fscn1
Relb
Il4il
Ccr7
Sirpa
Itgax
H2-DMb1
Cd209a
Naaa
Batf3
Clec9a
Xcr1
DC1
DC2
DC3
Average Expression
1.0
0.5
0.0
-0.5
-1.0
Percent Expressed
25
50
75
D
MC38 MerTK expression
WT
Axl -/-
UMAP 1
MerTK
E
B16F0-cOva MerTK expression
WT
Axl -/-
tSNE 1
tSNE 2
MerTK
F
Melanoma (OS)
HR = 1.46 (0.94 - 2.28)
logrank P = 0.091
Probability
Expression
low
high
Time (months)
Number at risk
low 397 327 245 161 104 57 13 0
high 141 101 71 50 29 11 4 0
G
PDAC (OS)
HR = 1.77 (1.14 - 2.73)
logrank P = 0.096
Probability
Expression
low
high
Time (months)
Number at risk
low 74 30 11 6 1
high 103 28 6 2 0

Fig. S1. Characterization of Axl and MerTK expression on tumor and myeloid cells. (**A**) Flow cytometry plots displaying levels of Axl expression on MC38, B16F0-cOva and Py8119-cOva cell lines. (**B**) Heatmap displaying canonical cell type markers used to annotate immune cell clusters. (**C**) Displaying immunophenotyping markers for cDC1, cDC2, and cDC3 subpopulations. (**D and E**) UMAP and TSNE projections showing MerTK expression levels in both WT and Axl KO mice across MC38 (**D**) and B16F0-cOva (**E**) tumor models respectively. (**F and G**) Kaplan-Meier curve illustrating the overall survival of melanoma (**F**) and pancreatic ductal adenocarcinoma (H) cancer patients stratified by low or high expression of Axl. P values were calculated by a log-rank Mantel-Cox test.

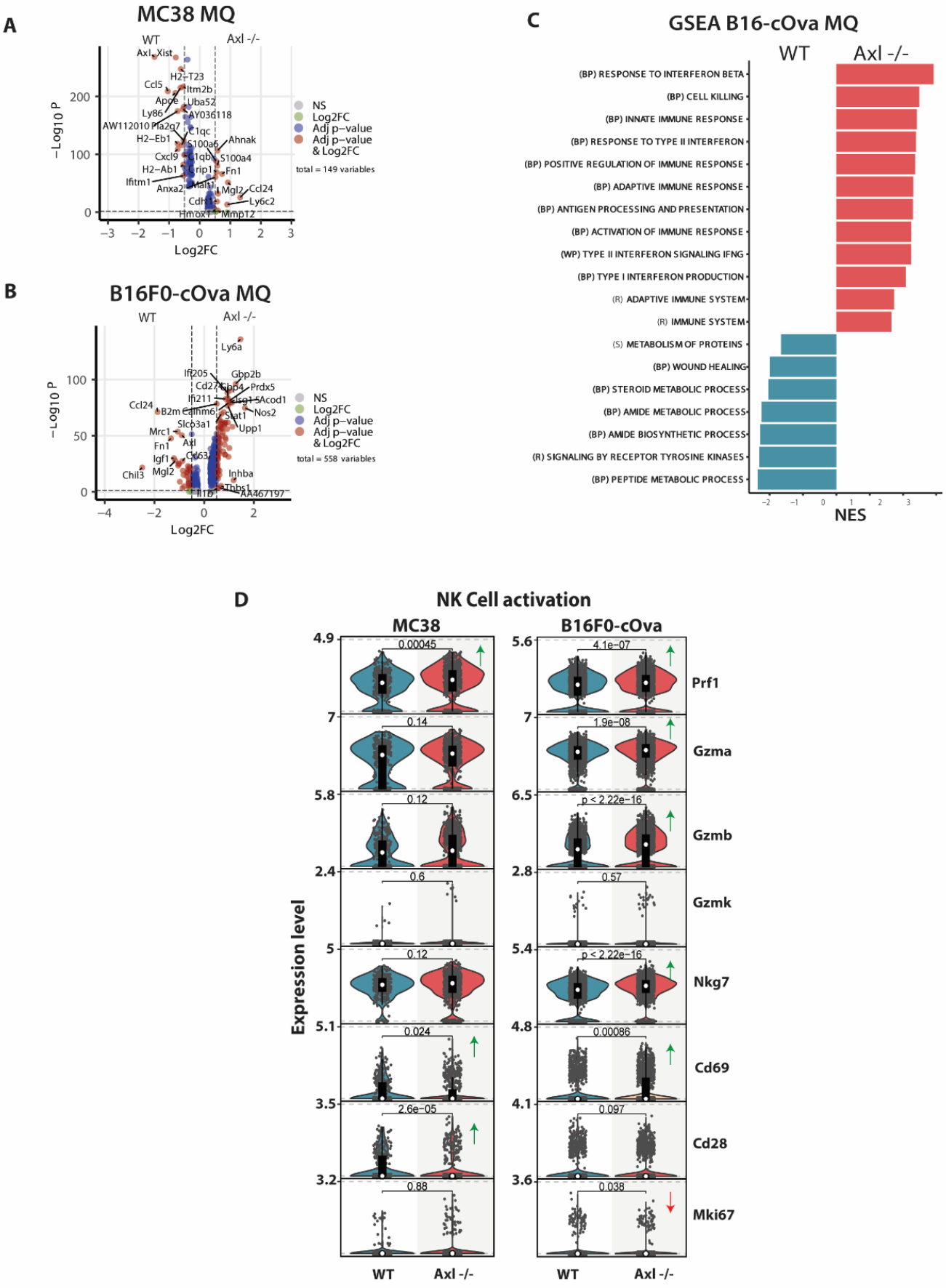
A
MC38 MQ
WT
Axl -/-
−Log10 P
Log2FC
NS
Log2FC
Adj p−value
Adj p−value & Log2FC
total = 149 variables
B
B16F0-cOva MQ
total = 558 variables
C
GSEA B16-cOva MQ
(BP) RESPONSE TO INTERFERON BETA
(BP) CELL KILLING
(BP) INNATE IMMUNE RESPONSE
(BP) RESPONSE TO TYPE II INTERFERON
(BP) POSITIVE REGULATION OF IMMUNE RESPONSE
(BP) ADAPTIVE IMMUNE RESPONSE
(BP) ANTIGEN PROCESSING AND PRESENTATION
(BP) ACTIVATION OF IMMUNE RESPONSE
(WP) TYPE II INTERFERON SIGNALING IFNG
(BP) TYPE I INTERFERON PRODUCTION
(R) ADAPTIVE IMMUNE SYSTEM
(R) IMMUNE SYSTEM
(S) METABOLISM OF PROTEINS
(BP) WOUND HEALING
(BP) STEROID METABOLIC PROCESS
(BP) AMIDE METABOLIC PROCESS
(BP) AMIDE BIOSYNTHETIC PROCESS
(R) SIGNALING BY RECEPTOR TYROSINE KINASES
(BP) PEPTIDE METABOLIC PROCESS
NES
D
NK Cell activation
MC38
B16F0-cOva
Expression level
Prf1
Gzma
Gzmb
Gzmk
Nkg7
Cd69
Cd28
Mki67
WT
Axl -/-

Fig. S2. Impact of Axl loss on macrophage and natural killer cells. (**A and B**) Volcano plot showing differentially expressed genes in intratumoral macrophages from WT or Axl-/- mice with MC38 (**A**) or B16F0-cOva (**B**) tumors (n=9193, 2759 cells respectively). (**C**) Plot illustrating the top gene sets enriched in intratumoral macrophages from WT or Axl-/- mice with B16F0-cOva tumors. Wikipathway = WP, Biological Process = BP, Reactome = R. (**D**) Violin plots comparing expression levels of activation markers on NK cells from WT and Axl KO mice in both MC38 and B16F0-cOva tumors.

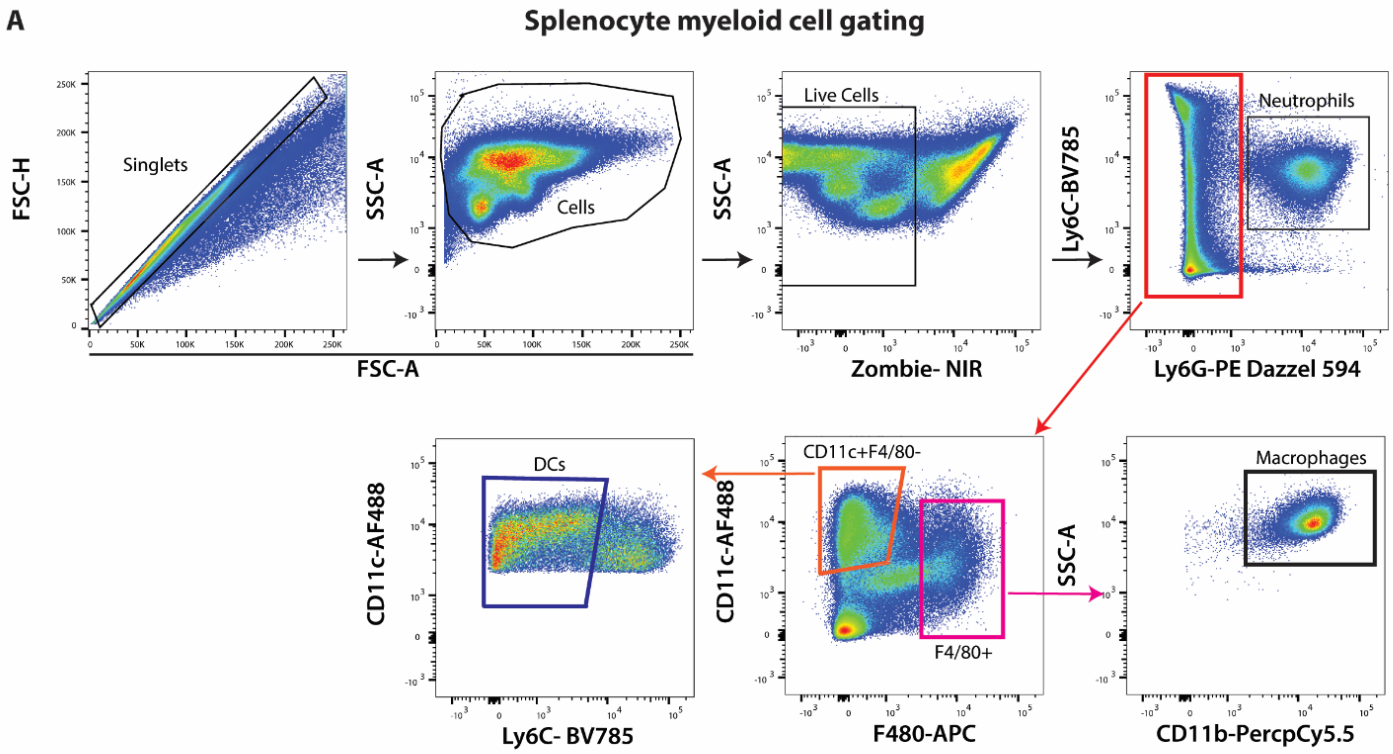

Fig. S3 (A) Flow cytometry gating strategy used to identify splenic myeloid cell populations found in mouse spleens.

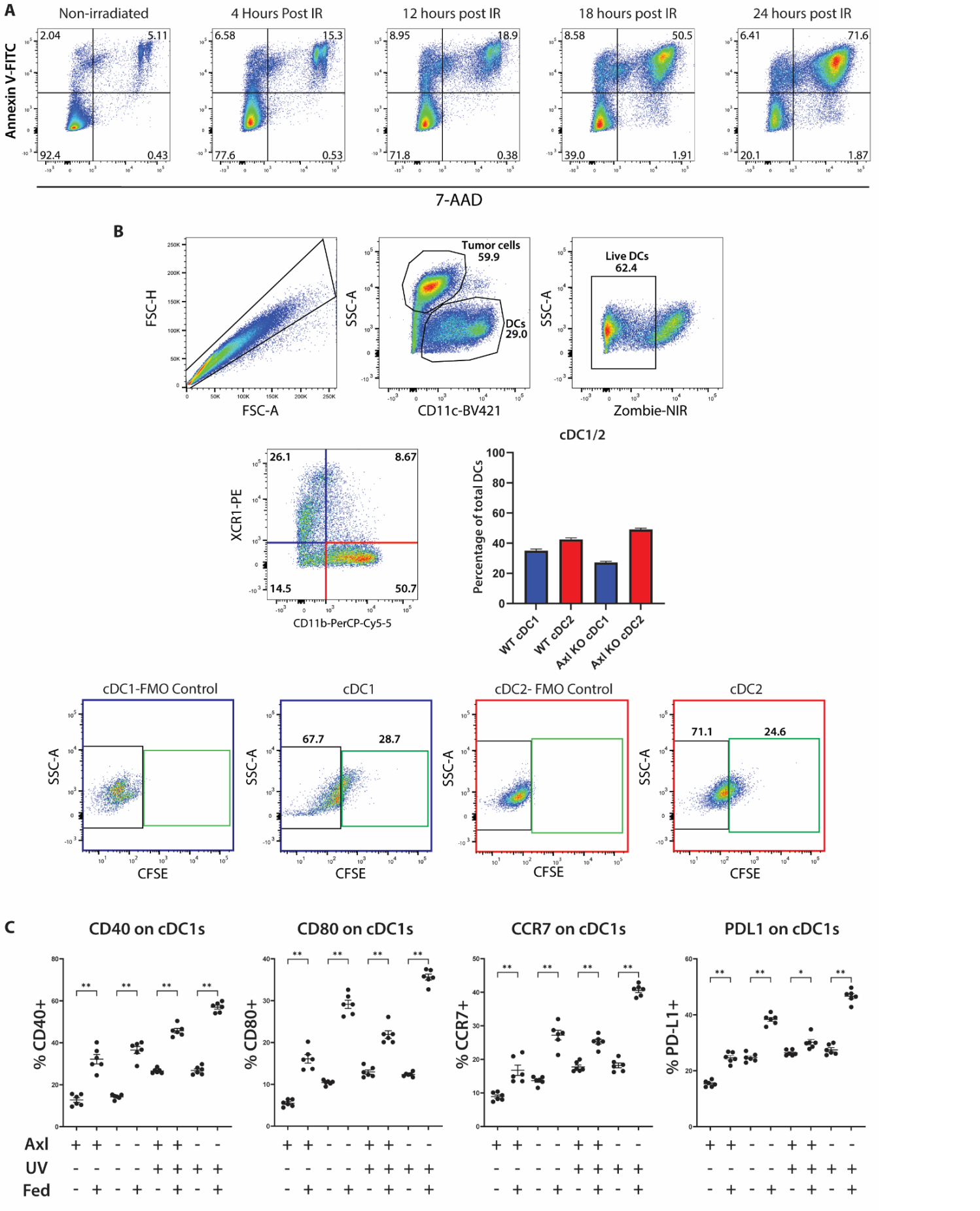
A
Non-irradiated
4 Hours Post IR
12 hours post IR
18 hours post IR
24 hours post IR
Annexin V-FITC
7-AAD
2.04
5.11
92.4
0.43
6.58
15.3
77.6
0.53
8.95
18.9
71.8
0.38
8.58
50.5
39.0
1.91
6.41
71.6
20.1
1.87
B
FSC-H
FSC-A
SSC-A
CD11c-BV421
Tumor cells
59.9
DCs
29.0
Live DCs
62.4
Zombie-NIR
XCR1-PE
CD11b-PerCP-Cy5-5
26.1
8.67
14.5
50.7
cDC1/2
Percentage of total DCs
WT cDC1
WT cDC2
Axl KO cDC1
Axl KO cDC2
cDC1-FMO Control
cDC1
cDC2- FMO Control
cDC2
CFSE
67.7
28.7
71.1
24.6
C
CD40 on cDC1s
CD80 on cDC1s
CCR7 on cDC1s
PDL1 on cDC1s
% CD40+
% CD80+
% CCR7+
% PD-L1+
Axl
UV
Fed

Fig. S4 Gating strategy and proportion of DC activation relative to UV treatment. (**A**) Flow cytometry plots showing apoptotic progression in B16F0-cOva cells following radiation treatment. (**B**) Flow cytometry gating strategy for identifying dendritic cells that have up taken tumor cell debris. (**C**) Graphs quantifying expression of activation markers presented as means +/- SEM on cDC1 cells. Here, "+ fed" and "– fed+ denote cDC1 cells that were positive or negative for CFSE fluorescence, indicating the uptake or absence of tumor cell debris, respectively. Each group consists of 6 technical replicates, significance was determined by one-way ANOVA followed by Tukey post hoc adjustment *P <0.05, **P <0.001.

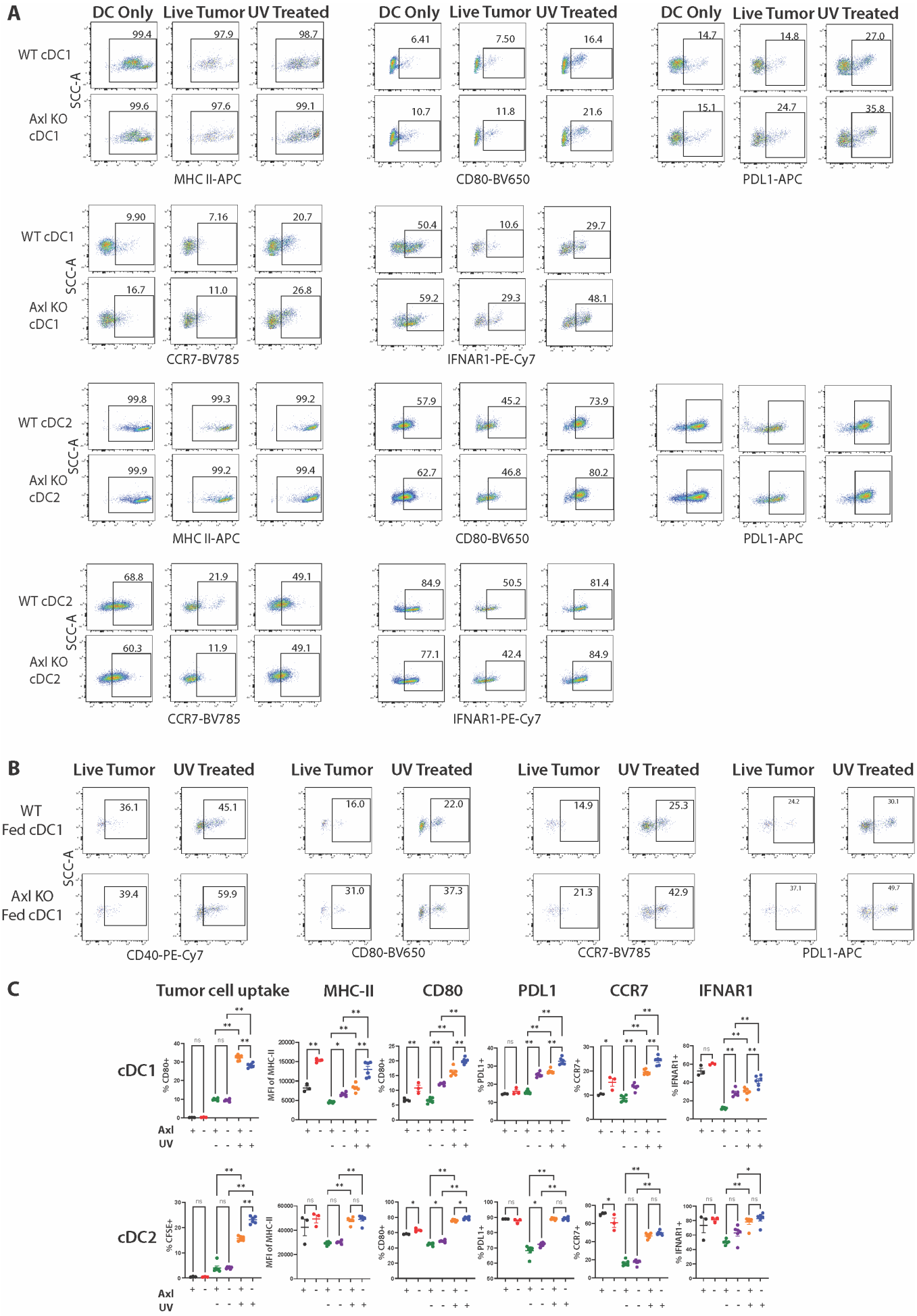
A
DC Only
Live Tumor
UV Treated
WT cDC1
Axl KO cDC1
SCC-A
99.4
97.9
98.7
99.6
97.6
99.1
MHC II-APC
6.41
7.50
16.4
10.7
11.8
21.6
CD80-BV650
14.7
14.8
27.0
15.1
24.7
35.8
PDL1-APC
9.90
7.16
20.7
16.7
11.0
26.8
CCR7-BV785
50.4
10.6
29.7
59.2
29.3
48.1
IFNAR1-PE-Cy7
WT cDC2
Axl KO cDC2
99.8
99.3
99.2
99.9
99.2
99.4
MHC II-APC
57.9
45.2
73.9
62.7
46.8
80.2
CD80-BV650
PDL1-APC
68.8
21.9
49.1
60.3
11.9
49.1
CCR7-BV785
84.9
50.5
81.4
77.1
42.4
84.9
IFNAR1-PE-Cy7
B
Live Tumor
UV Treated
WT Fed cDC1
Axl KO Fed cDC1
SCC-A
36.1
45.1
39.4
59.9
CD40-PE-Cy7
16.0
22.0
31.0
37.3
CD80-BV650
14.9
25.3
21.3
42.9
CCR7-BV785
24.2
30.1
37.1
49.7
PDL1-APC
C
Tumor cell uptake
MHC-II
CD80
PDL1
CCR7
IFNAR1
cDC1
cDC2
% CD80+
MFI of MHC-II
% CD80+
% PDL1+
% CCR7+
% IFNAR1+
% CFSE+
MFI of MHC-II
% CD80+
% PDL1+
% CCR7+
% IFNAR1+
Axl
UV
ns
*
**

Fig. S5 cDC1 and cDC2 maturation marker expression in WT and Axl KO mice. (**A**) Representative flow cytometry plots of MHC-II, CD80, PD-L1, CCR7, and IFNAR1 on WT and Axl KO cDC1 (top two rows) and cDC2 (bottom two rows) cultured alone, with live tumor cells, or with UV-irradiated tumor cells. Gated numbers indicate the percentage of marker-positive cells. (**B**) Representative flow cytometry plots of CD40, CD80, CCR7, and PD-L1 on fed ($CFSE^+$, debris-engulfing) WT and Axl KO cDC1 cultured with live or UV-irradiated tumor cells. (**C**) Quantification of tumor cell uptake (% $CFSE^+$), MHC-II expression (median fluorescence intensity), and the frequency of $CD80^+$, $PD\text{-}L1^+$, $CCR7^+$, and $IFNAR1^+$ cells among cDC1 (top) and cDC2 (bottom) from WT (Axl^+) and Axl KO (Axl^-) mice cultured alone (DC Only), with live tumor cells (UV −), or with UV-irradiated tumor cells (UV +). Each symbol represents an individual biological replicate; bars show mean ± SEM. Statistical significance was determined by one-way ANOVA with Tukey's multiple-comparisons test; ns, not significant; $P < 0.05$, $^{**}P < 0.001$.

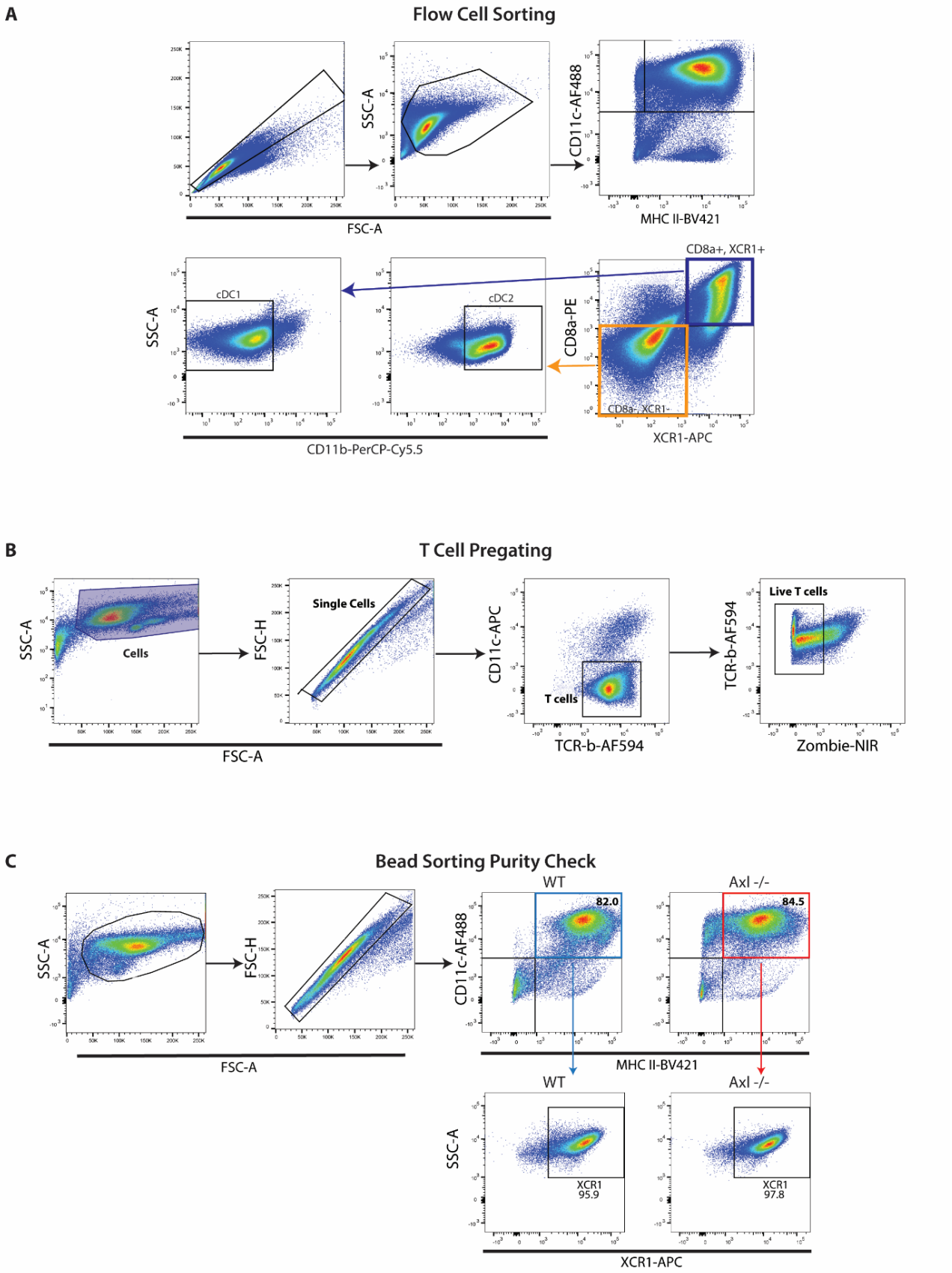

Fig. S6 Sorting of cells for adoptive transfer. (**A)** Flow cytometry plots depicting the flow sorting strategy for splenic DC1 and DC2 cells. **(B)** Flow cytometry plots illustrating OTI CD8+ T cell pre-gating strategy. (**C**) Flow cytometry plots depicting cell purity post DC1 bead sorting.